COMPUTER PROCESSING AND MODELING – Communication

Magnetic Resonance in Medicine 68:278–285 (2012)

Fast Joint Design Method for Parallel Excitation Radiofrequency Pulse and Gradient Waveforms Considering Off-Resonance

Daehyun Yoon,[1]* Jeffrey A. Fessler,[1,2] Anna C. Gilbert,[3] and Douglas C. Noll[2]

A fast parallel excitation pulse design algorithm to select and to order phase-encoding (PE) locations (also known as "spokes") of an Echo-Volumar excitation *k*-space trajectory considering B_0 field inhomogeneity is presented. Recently, other groups have conducted research to choose optimal PE locations, but the potential benefit of considering B_0 field inhomogeneity during PE location selection or their ordering has not been fully investigated. This article introduces a novel fast greedy algorithm to determine PE locations and their order that takes into account the off-resonance effects. Computer simulations of the proposed algorithm for B_1 field inhomogeneity correction demonstrate that it not only improves excitation accuracy but also provides an effective ordering of the PE locations. Magn Reson Med 68:278–285, 2012. © 2012 Wiley Periodicals, Inc.

Key words: parallel excitation; RF pulse design; PE location selection; spoke selection; EV trajectory

INTRODUCTION

Trains of slice-selective pulses are useful for designing slice-selective parallel excitation radiofrequency (RF) pulses (1,2). This approach has been successfully applied to B_1 field inhomogeneity correction (3–5), signal recovery for blood oxygenation level dependent functional magnetic resonance imaging (6–8), spatial-spectral excitation (9), and large tip-angle multidimensional excitation (10,11). In this framework, each RF coil transmits a train of weighted slice-selective pulses interleaved by in-plane gradient blips to achieve a required in-plane excitation profile. Determining the RF pulse requires computing only one scalar weight per slice-selective pulse for each transmission coil. Therefore, it significantly reduces the number of unknown RF parameters compared with conventional tailored RF pulse designs (12,13), where the RF pulse is sampled finely in time (a few μs), yielding thousands of RF pulse samples to compute.

In the above pulse design approach, one must jointly compute the best pulse weights and in-plane gradient waveforms. The cost function for optimization often uses the excitation *k*-space analysis for the small tip-angle domain (14), where in-plane gradient waveform optimization becomes equivalent to optimizing phase-encoding (PE) locations (also denoted as "spokes") of an Echo-Volumar (EV) trajectory in excitation *k*-space (1). As the number of PE locations equals the number of slice-selective pulses in the resulting pulse train, sparse selection is crucial to limit the final RF pulse length. Recently, (3,4) presented a convex optimization approach adopting an $l1$-norm based penalty to enforce sparsity of the selected PE locations. However, this method can be slow, so other schemes have been developed to accelerate PE location selection. For example, iterative greedy approaches (5,15,16) based on orthogonal matching pursuit (17) or sequential selection (18) achieved excitation accuracy similar to the convex optimization scheme with much less computation.

However, none of the aforementioned methods implemented PE location selection and ordering process considering off-resonance effects. In (5), a model considering off-resonance was suggested but detailed implementation results were not provided. In this article, we show via computer simulation that considering off-resonance when selecting PE locations can improve excitation accuracy. We demonstrate that heuristics for ordering PE locations, such as shortest-path (4,5) or spiral-in (8,19), can be quite suboptimal in some cases. We describe a novel greedy algorithm for determining PE locations that considers B_0 field inhomogeneity during PE location selection. Our algorithm is a fast greedy selection process based on (16) that chooses PE locations sequentially in a time-reversed order, which naturally yields an effective ordering of the selected PE locations. In our PE location selection process, the basis signal associated with each PE location is modulated by the off-resonance phase accrual, allowing more accurate modeling than previous greedy methods (5,15,16). Computer simulations show that our method achieves higher excitation accuracy than conventional methods in significantly less computation time. At the time of preparing this work, our parallel transmission hardware was not stable enough to run our pulse design, so our scope is limited to provide simulation data. At 3 T where our simulation experiments are proposed, the shape of the B_1 fields should not vary by large amount with different coil loading, so we believe that our results illustrate the potential benefits of our proposed algorithm.

[1]Department of Electrical Engineering and Computer Science, University of Michigan, Ann Arbor, Michigan, USA.
[2]Department of Biomedical Engineering, University of Michigan, Ann Arbor, Michigan, USA.
[3]Department of Mathematics, University of Michigan, Ann Arbor, Michigan, USA.

Grant sponsor: National Institutes of Health; Grant number: 5R01NS058576-03.

*Correspondence to: Daehyun Yoon, M.S., 2360 Bonisteel Ave., Ann Arbor, MI 48109-2108. E-mail: quann@umich.edu

Received 29 November 2011; revised 28 March 2012; accepted 3 April 2012.
DOI 10.1002/mrm.24311
Published online 3 May 2012 in Wiley Online Library (wileyonlinelibrary.com).

THEORY

Optimization Formulation

We assume a small-tip angle RF pulse sequence where the RF pulse train is composed of M slice-selective RF pulses from L transmission coils. The mth slice selective pulse from the lth coil is a slice-selective basis pulse weighted by a complex scalar, $\alpha_l(m)$, that we determine through optimization. Using the excitation k-space analysis for a small-tip angle domain (14), we approximate the final excitation pattern as follows:

$$d(x,y,z) \approx b(z) \times \sum_{l=1}^{L}\sum_{m=1}^{M} s_l(x,y)\alpha_l(m)e^{i2\pi\left(xk_x(m)+yk_y(m)\right)}e^{i2\pi\Delta\omega(x,y)(t_m-T)}. \quad [1]$$

Herein, the excited pattern has a separable form. The through-plane excitation profile is $b(z)$ from the slice-selective basis pulse and the in-plane profile is determined by the terms in the double summation. $\Delta\omega(x, y)$ is the B_0 fieldmap, t_m is the time corresponding to the middle of the mth slice-selective pulse, and T is the end time of the RF pulse sequence. $(k_x(m), k_y(m))$ is the mth PE location in the EV trajectory obtained by running time-reversed integral of the in-plane gradient waveforms. For optimization, we first design the PE locations and then derive corresponding gradient waveforms considering the hardware limitations. We assumed that the slice-profile is thin enough that the lth transmission coil's sensitivity, $s_l(x, y)$, can be approximated as a two-dimensional pattern (disregarding its through-plane variation). Note that a similar model was suggested in the Appendix of (5) without presenting implementation results.

The goal of our proposed RF pulse design algorithm is to jointly optimize RF pulse weights and PE locations to achieve a desired in-plane excitation pattern, $\boldsymbol{\theta}(x,y)$. The cost function for our optimization problem is described as a following matrix-vector form:

$$\min_{\alpha_l(m),\mathbf{f}_m}\left\|\boldsymbol{\theta}-\sum_{l=1}^{L}\sum_{m=1}^{M}\mathbf{S}_l\mathbf{W}_m\mathbf{f}_m\alpha_l(m)\right\|_2^2 \equiv \min_{\boldsymbol{\alpha},\mathbf{f}_m}\|\boldsymbol{\theta}-\mathbf{A}\boldsymbol{\alpha}\|_2^2$$
$$\text{where } \mathbf{A}=[\mathbf{S}_1\mathbf{W}_1\mathbf{f}_1,\mathbf{S}_2\mathbf{W}_1\mathbf{f}_1,\ldots,\mathbf{S}_L\mathbf{W}_1\mathbf{f}_1,\mathbf{S}_1\mathbf{W}_2\mathbf{f}_2,\ldots,\mathbf{S}_L\mathbf{W}_M\mathbf{f}_M],\ \text{and}\ \boldsymbol{\alpha}=[\alpha_1(1),\ldots,\alpha_L(M)]^{\mathrm{T}}. \quad [2]$$

$\boldsymbol{\theta}$ is a column vector containing the spatial samples of $\boldsymbol{\theta}(x,y)$, $\mathbf{S}_l$ is a diagonal matrix of spatial samples of the lth coil's sensitivity, $s_l(x,y)$, $\mathbf{W}_m$ is a diagonal matrix of spatial samples of the off-resonance phase, $e^{i2\pi\Delta\omega(x,y)(t_m-T)}$, and $\mathbf{f}_m$ is a column vector of spatial samples of a two-dimensional complex exponential, $e^{i2\pi(xk_x(m)+yk_y(m))}$. In this minimization problem, we attempt to choose optimal PE locations from a set of candidate PE locations formed by sampling two-dimensional excitation k-space at Nyquist rate. The number of PE locations, M, should be limited to yield a RF pulse of reasonable length. For this purpose, we seek the minimum M having acceptable excitation accuracy. Therefore, M is not a prefixed parameter for the optimization though it does not explicitly appear in the optimization parameter set.

Optimization Strategy

Our greedy algorithm is an iterative procedure, where PE locations are selected in a time-reversed order. During the mth iteration, we select the mth from the last PE location. We use this order to determine the off-resonance phase accrual, $\Delta\omega(x,y,z)(t_m - T)$, without prespecifying the number of selected PE locations, M, and the corresponding RF pulse train length, T. We increment the parameter M, after each iteration in the optimization, so its final value is known only after the optimization is finished. However, the off-resonance phase accrual is well defined when we compute it in the time-reversed order regardless of M because $(t_m - T)$ becomes known instead. The reverse sequential selection also allows us to precisely control the trade-off between the number of selected PE location and the excitation accuracy.

Let $E(N)$ denote the list of (ordered) PE locations, $\{(k_x(1),k_y(1)), (k_x(2),k_y(2)),\ldots, (k_x(N),k_y(N))\}$, determined after N iterations in our algorithm. In the next iteration, we seek to choose from a discrete set of candidates the PE location that most reduces the cost function when "added" to the list $E(N)$. The new PE location is added to the front of the list, yielding a new list $E(N + 1)$. For a given list of PE locations, $E(N)$, we minimize the cost function in Eq. 2 by performing the orthogonal projection of the desired excitation pattern $\boldsymbol{\theta}$ onto the basis generated by the chosen PE locations, $\{\mathbf{S}_1\mathbf{W}_1\mathbf{f}_1,\ldots, \mathbf{S}_L\mathbf{W}_N\mathbf{f}_N\}$.

Whereas the method in (5) used orthogonal projection for every candidate, here we investigated a simple greedy method that uses significantly fewer orthogonal projections. In Eq. 2, the in-plane variation of the excited pattern is synthesized linearly by the basis signals associated with the chosen PE locations. This implies that an effective candidate PE location has associated basis signals that are highly correlated with $\boldsymbol{\theta}(x,y)$. With L transmission coils, selecting one frequency, $\mathbf{f}$ for the mth PE location produces L basis signals, $\{\mathbf{S}_1\mathbf{W}_m\mathbf{f},\ldots, \mathbf{S}_L\mathbf{W}_m\mathbf{f}\}$. Inspired by the sum of correlations criterion presented in (20), we devised a cumulative correlation criterion to estimate how much one candidate PE location contributes to spanning the excitation pattern (or its projection residual after the first iteration). It is defined as a simple sum of squares of correlation values between the individual basis and the target pattern, $\mathbf{r}$, as follows:

$$\sum_{l=1}^{L}|\langle\mathbf{r},\mathbf{S}_l\mathbf{W}_\mathbf{m}\mathbf{f}\rangle|^2. \quad [3]$$

We normalized each sensitivity pattern with respect to its $l2$ norm before computing the correlation to avoid any bias toward sensitivity patterns of higher norm. In using the cumulative correlation, we hope that the sensitivity patterns are reasonably localized such that they do not overlap "too much." Then, summing the correlation with the basis signal for each coil can reasonably approximate the magnitude of the target pattern projected onto the range space of the basis signals. We compute this cumulative correlation between each candidate and the projection residual from the previous iteration to cull only a few effective candidates for which we run orthogonal projections. The culling process greatly reduces the computation time spent in running orthogonal

Table 1
The Detailed Procedures of the Proposed Algorithm

Problem description
$\min_{\boldsymbol{\alpha},\mathbf{f}_m} \|\mathbf{r}\|_2^2$ where $\mathbf{r} = \boldsymbol{\theta} - \mathbf{A}\boldsymbol{\alpha}$, $\mathbf{A} = [\mathbf{S}_1\mathbf{W}_1\mathbf{f}_1, \ldots, \mathbf{S}_L\mathbf{W}_M\mathbf{f}_M]$, and $\boldsymbol{\alpha} = [\alpha_1(1), \ldots, \alpha_L(M)]^{\mathrm{T}}$

Solution approach
No PE location is chosen initially. To try to minimize $\|\mathbf{r}\|$, the PE locations are chosen sequentially in a time-reversed order from a set of candidate PE locations.

Variable notation
For an ordered list of PE location, $E = \{(k_x(1),k_y(1)), (k_x(2),k_y(2)), \ldots, (k_x(N),k_y(N))\}$, a matrix $\mathbf{A}_E$ is defined as $\mathbf{A}_E = [\mathbf{S}_1\mathbf{W}_1\mathbf{f}_1, \ldots, \mathbf{S}_L\mathbf{W}_N\mathbf{f}_N]$, where $\mathbf{f}_n$ is a column vector of spatial samples of a two-dimensional complex exponential, $e^{i2\pi(xk_x(n)+yk_y(n))}$. $\mathbf{S}$ and $\mathbf{W}$ are matrices containing the coil sensitivity and the off-resonance phase samples, respectively, as defined in the Theory section.

Algorithm
Initialize the list of the chosen PE location, E, as an empty list.
Initialize the excitation residual, $\mathbf{r} = \boldsymbol{\theta}$, as the target in-plane excitation pattern.
Define the set of possible candidate PE locations, F, by sampling two-dimensional excitation k-space at Nyquist rate.
$\mathbf{f}_n$ vectors above will be instantiated from the candidate PE locations contained in F.
Initialize the set of culled candidate PE locations, C, as an empty set.

Loop until $\|\mathbf{r}\|$ is sufficiently small or the number of selected PE locations reaches a limit {
  Step 1: Cull effective PE locations from F, and add them to C.
    Find p candidates in F having the highest cumulative correlation with $\mathbf{r}$ using Eq. 3.
    Add those p candidates to C.
  Step 2: Find the PE location in C that best reduces $\|\mathbf{r}\|$.
    For each candidate in C, create a new list E' by prepending it to E.
    Compute the residual of orthogonal projection of $\boldsymbol{\theta}$ onto $\mathbf{A}_{E'}$, which is $\boldsymbol{\theta} - (\mathbf{A}_{E'}^{\mathrm{h}}\mathbf{A}_{E'})^{-1}\mathbf{A}_{E'}^{\mathrm{h}}\boldsymbol{\theta}$
    Find the candidate with the minimum residual.
  Step 3: Select the PE location found in Step 2 as the mth from the last PE location.
    Add the candidate found in Step 2 to the front of E.
  Step 4: Update other parameters.
    Pulse weights : $\boldsymbol{\alpha} = (\mathbf{A}_E^{\mathrm{h}}\mathbf{A}_E)^{-1}\mathbf{A}_E^{\mathrm{h}}\boldsymbol{\theta}$
    $\mathbf{r} = \boldsymbol{\theta} - (\mathbf{A}_E^{\mathrm{h}}\mathbf{A}_E)^{-1}\mathbf{A}_E^{\mathrm{h}}\boldsymbol{\theta}$
    Discard PE locations in C except those with p smallest $\|\mathbf{r}\|$ values
}
Our algorithm becomes equivalent to the modification of (5) if C is replaced with the set of entire candidates, F in Step 2.

projections. To implement the orthogonal projection, we adopted the fast numerical scheme proposed in (5).

The details of our algorithm are presented in Table 1. At each iteration of our algorithm, the correlation test based on Eq. 3 identifies p candidate PE locations that are added to a set of effective candidates denoted as C in Table 1. We select the design parameter p before the optimization; using a larger p may achieve better excitation accuracy at the expense of computation time. Before this addition, the set C already has p candidates retained from the previous iteration. For each of these $2p$ candidates in C, we run the orthogonal projection test by minimizing Eq. 2. In other words, we compute the orthogonal projection of the desired excitation pattern onto the basis signals specified by the candidate and the previously established PE locations. We select the candidate PE location that best spans the desired excitation pattern and added it to the list of chosen PE locations. After that, we retain only the p candidates having the smallest projection errors and remove the rest from C. Selecting multiple candidates in the correlation test and passing some of them to the next iteration compensates for the imperfections in using the cumulative correlation as a measure of the effectiveness of one candidate for the subsequent orthogonal projection.

METHODS

Test Application Description

We applied our algorithm to B_1 field inhomogeneity correction (3–5). The goal of the RF pulse design here is to compute an effective RF pulse that excites a uniform in-plane profile. The in-plane profile, $\boldsymbol{\theta}$, in Eq. 2 is 1 in the excitation region of interest. In human brain scans, the air space outside the head corresponds to the "don't care" region, so the norm in Eq. [2] is taken only within the head. For comparison with our proposed method, we implemented three other methods: the convex method (4), the greedy method (5), and the greedy method extended to consider off-resonance during PE location selection briefly suggested in (5). As the extension of (5) did not describe a specific ordering of the chosen PE locations, we implemented it with our sequential selection in a time-reversed order.

Assessment Criteria

To investigate how much ordering can affect the excitation accuracy in the presence of high off-resonance, we first tried every possible ordering of selected PE locations from the convex method (4) and the greedy method (5) that uses a heuristic ordering scheme (shortest-path). We measured the Normalized Root Mean Squared Error

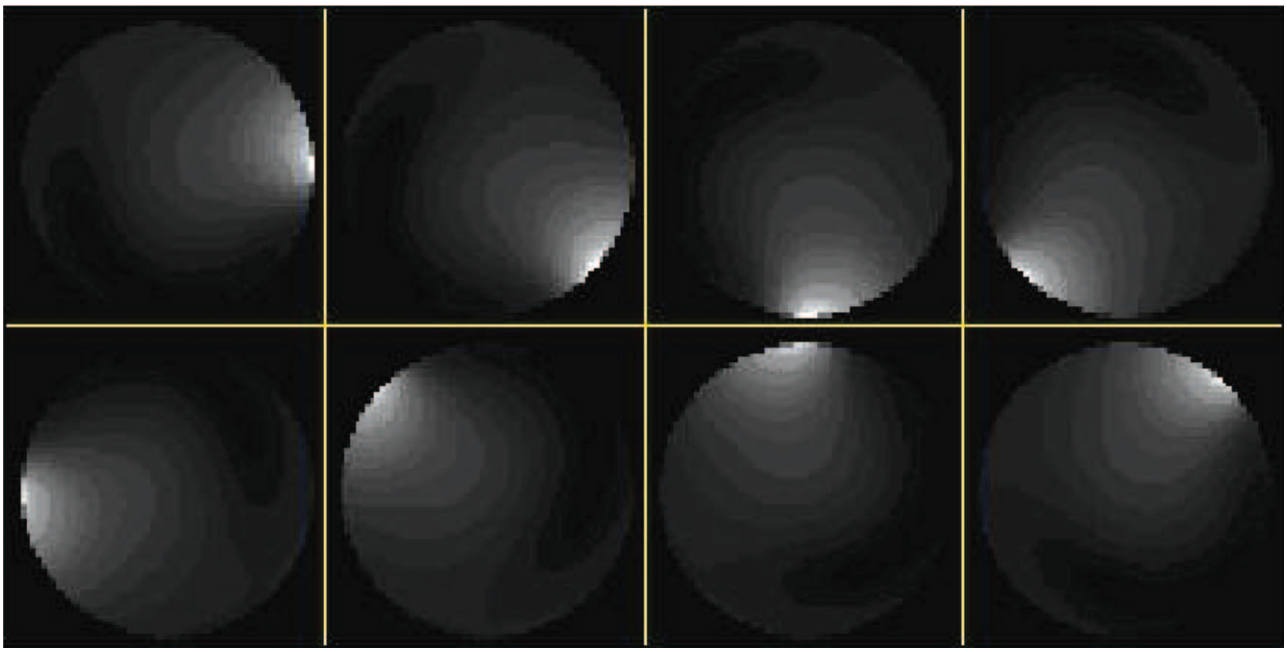

FIG. 1. Magnitude images of sensitivity patterns of eight-channel transmission coils used in simulation experiments. [Color figure can be viewed in the online issue, which is available at wileyonlinelibrary.com.]

(NRMSE) of the achieved in-plane excitation pattern. We compared these errors with those of our method and the aforementioned modification of (5). Because the number of possible ordering is the factorial of the number of selected PE locations, we focused on the case that five PE locations are chosen. Also, we recorded the computation time of all methods to test whether they can satisfy practical on-line computation requirements.

Experiment Parameters

We conducted simulation studies to compare aforementioned algorithms. They were implemented with Matlab (MathWorks, Natick, MA) on a computer with Intel Q6600 CPU at 2.4 GHz and 4 GB RAM. The sensitivity patterns of an eight channel active rung transmit array (21) were obtained by Finite-Difference Time-Domain simulation (22) at 3 T, where we assumed a phantom of a 22 cm diameter lossy cylinder with $\sigma = 0.3$ S/m and $\varepsilon_r = 80$. Figure 1 shows the simulated transmission sensitivity patterns. The B_0 fieldmap and the excitation region of interest (ROI) were acquired from in vivo human brain scans for two subjects. We chose two 5-mm thick axial slices of relatively high off-resonance for the RF pulse design. The excitation field of view was 24 cm $\times$ 24 cm with 64 $\times$ 64 uniform sampling grid specifying the desired excitation pattern. The candidate PE locations were formed by sampling the continuous in-plane frequency space at the Nyquist rate. For our proposed method, we used the full set of 64^2 candidates but only 19 $\times$ 19 low frequency candidates were used for the other methods as suggested in their original studies. The desired flip angle was 10°. A Hanning-windowed sinc pulse with one side lobe was used for the basis pulse, which was 0.75 ms long due to the current gradient hardware limitations, where the slew rate of the gradient was 150 T/m/s and the maximum gradient amplitude was 4 g/cm.

RESULTS

Ordering of PE Locations and Excitation Accuracy

Figure 2 illustrates the B_0 fieldmaps and the excitation ROI of chosen brain slices. The air cavity regions in the

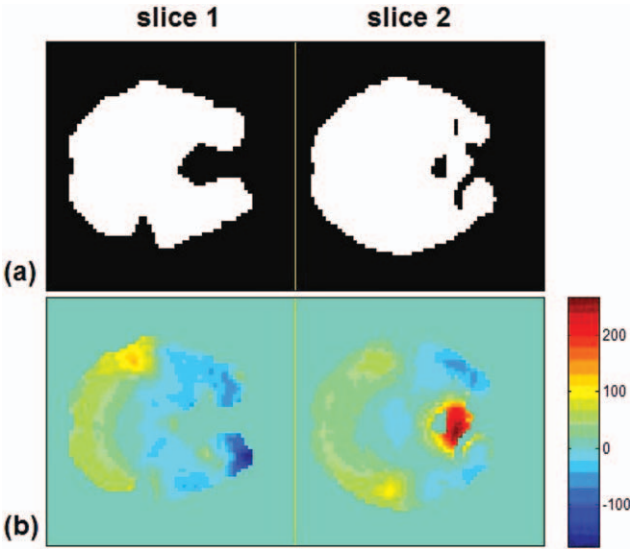

FIG. 2. Excitation ROI (**a**) and B_0 fieldmap (**b**) of two axial slices acquired from human scans. In the excitation ROI, the desired excitation pattern is set to be 1 in the white area, and "don't care" in the black area. The units of the fieldmap are Hz. The B_0 fieldmaps shows very high off-resonance frequencies due to susceptibility difference around air cavity regions such as ear canals and a frontal sinus. [Color figure can be viewed in the online issue, which is available at wileyonlinelibrary.com.]

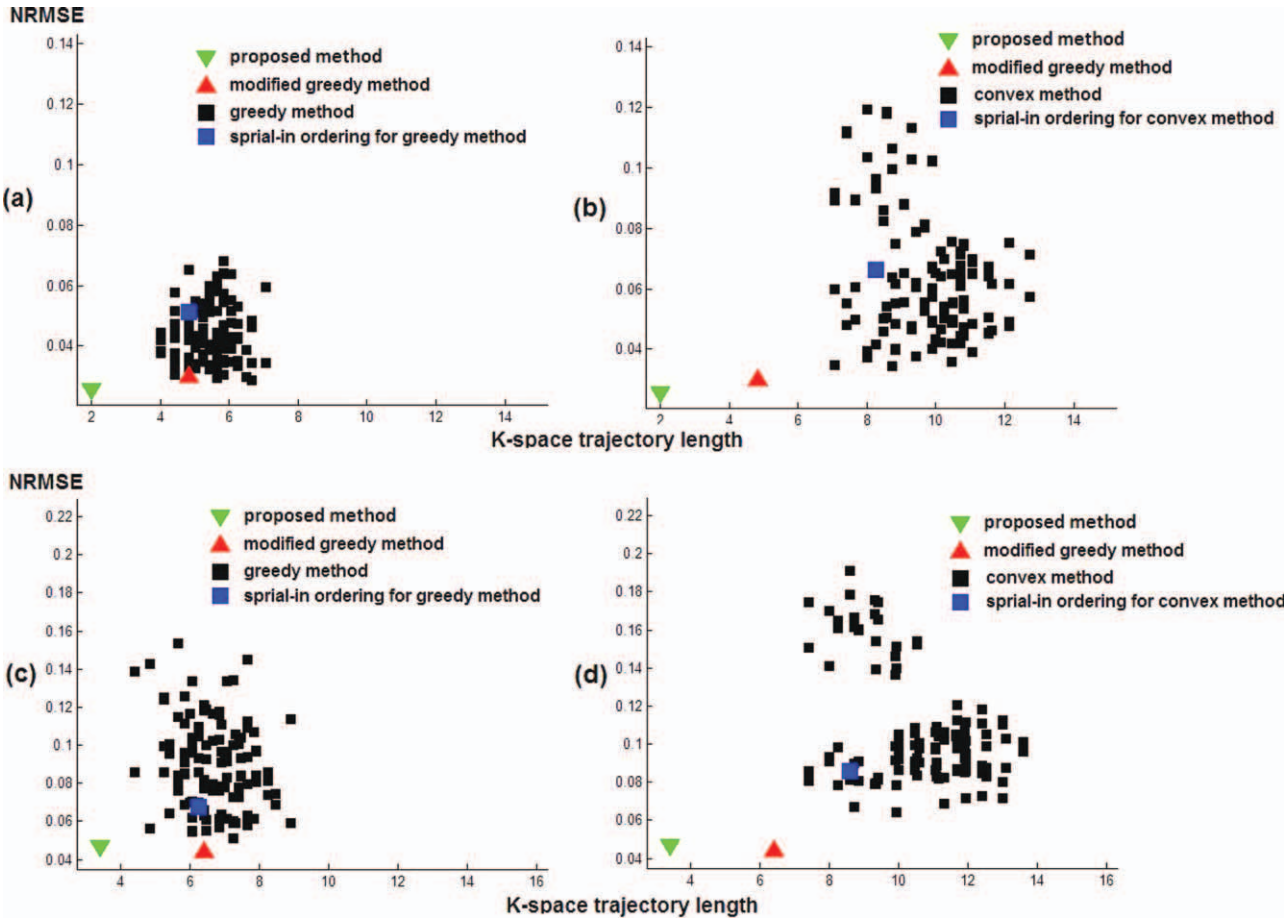

FIG. 3. Scatter plots of NRMSE versus the length of EV *k*-space trajectory obtained with different PE location orderings. **a**, **c**: Different orderings of PE locations with the greedy method applied for slices 1 and 2, respectively. **b**, **d**: With the convex method for slices 1 and 2, respectively. A black square mark indicates a PE ordering from the convex method or the greedy method. A blue square mark is for the spiral-in ordering of PE locations obtained from the convex method or the greedy method. Conventional heuristic approaches to connect PE locations such as the shortest-path or the spiral-in did not show obvious optimal excitation accuracy. Our method and the modification of the greedy method consistently tend to show improved excitation accuracy than the compared conventional methods. [Color figure can be viewed in the online issue, which is available at wileyonlinelibrary.com.]

slices caused high off-resonance frequencies ranging from −150 Hz to 200 Hz. Figure 3 plots the NRMSE of different PE location orderings for the convex method and for the greedy method along the associated EV trajectory length. The results from our method and the modification of (5) are marked as well. Note that our method and the modification of (5) do not use the same PE locations as the compared methods. Figure 3 demonstrates that our method and the modification of (5) generally have lower excitation error than any PE location ordering for the compared methods. There is no obvious relationship between the *k*-space trajectory length and the resulting excitation error. Even within the shortest orderings, there were considerable NRMSE variations in some cases. Also, connecting the PE locations in a spiral-in manner for the convex and the greedy method failed to achieve optimal excitation accuracy.

Uniformity of In-Plane Excitation Profiles

To visually assess the uniformity of the excited in-plane profile, we ran the Bloch simulation of RF pulses computed for slice 2 and plotted the resulting in-plane excitation patterns and the corresponding PE locations in Fig. 4. To represent multiple shortest-path PE location orderings of the convex method and the greedy method, both the minimum NRMSE case and the maximum NRMSE case were displayed. The transverse magnetization profiles at the center of the slice ($z = 0$) were simulated. To quantify the uniformity of the excitation profile, we calculated the mean and the standard deviation (σ) of the transverse magnetization magnitude for each pulse design. The in-plane excitation patterns in Fig. 4 show that our proposed method and the modification of (5) outperformed both the convex and the greedy method with respect to the uniformity. For example, σ of the minimum NRMSE case with convex method was the most uniform among the cases with the convex and the greedy method, but it was still 1.6 times larger than that of our method and the modification of (5). The difference in the uniformity becomes even more dramatic when our method is compared with the maximum NRMSE case of the convex and the greedy method. In that case, their σs were three times and 2.6 times larger than that of our method, respectively.

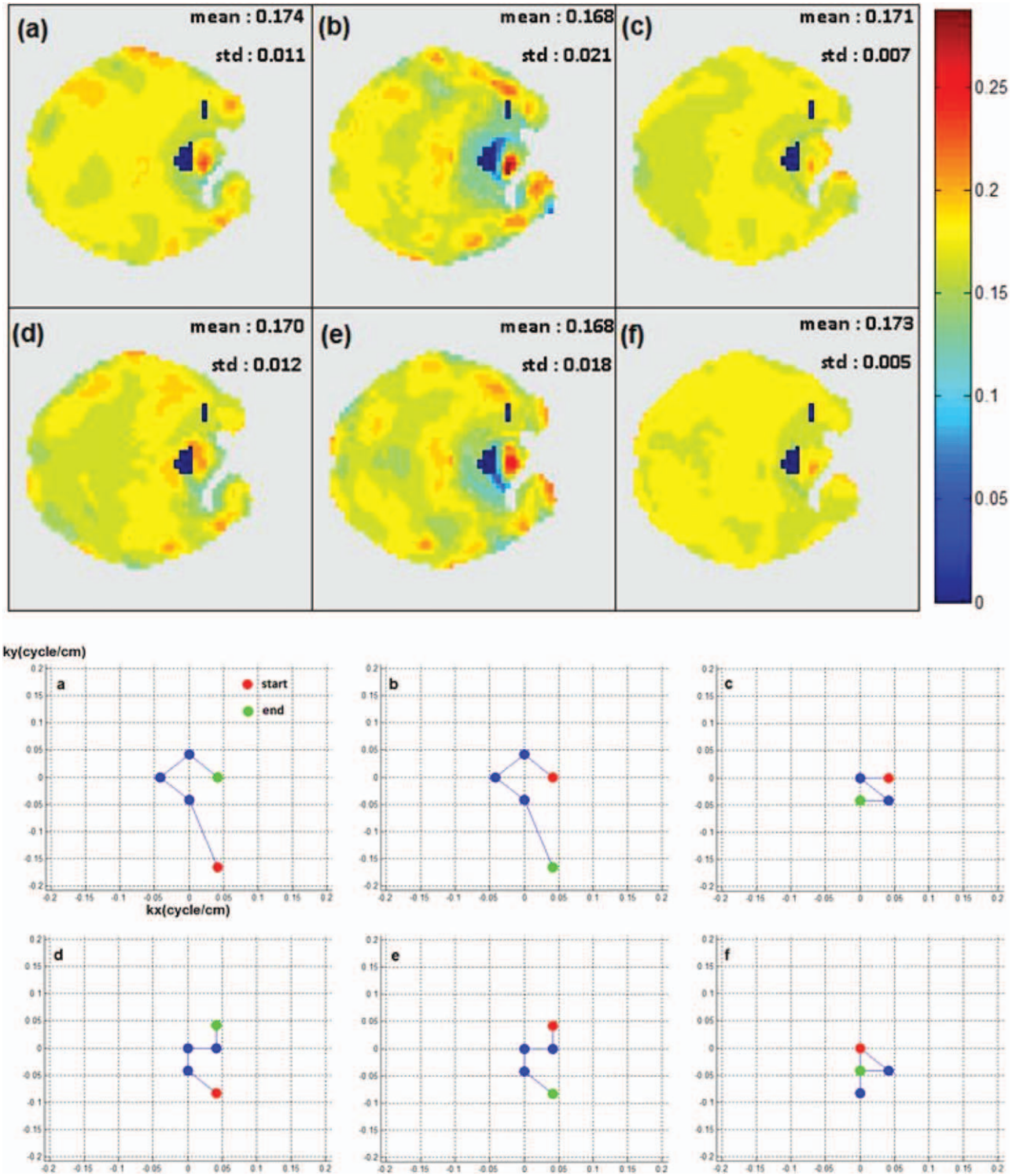

FIG. 4. Uniformity of the in-plane excitation pattern simulated with different methods for slice 2. In-plane excitation profiles at $z = 0$ and corresponding PE locations and their ordering. **a**: The minimum NRMSE case with the shortest-path ordering with the convex method, (**b**) the maximum NRMSE case with the shortest-path ordering with the convex method, (**c**) our proposed method, (**d**) the minimum NRMSE case of with the shortest-path ordering with the greedy method, (**e**) the maximum NRMSE case of with the shortest-path ordering with the greedy method, (**f**) modification of the greedy method. Our proposed method and the modified greedy method show more uniform profiles than others.

Table 2
Computation Time of Different Pulse Design Methods for Each Slice

Slice	Convex method	Greedy method	Modified greedy method	Proposed method
1	1434.0 s	5.7 s	7.9 s	0.9 s
2	1729.4 s	5.4 s	5.3 s	0.3 s

We used each method to determine five PE locations to create a uniform excitation pattern for each slice. The computation time varies between different slices because depending on the size of the ROI, the number of spatial samples for the excitation pattern changes. Our method is by far the fastest method, whereas the convex method is the slowest. The greedy method runs reasonably fast, but our method is still almost an order of magnitude faster.

Computation Time

Table 2 summarizes the computation time taken by each method for selecting PE locations. The convex optimization takes the longest time, as reported previously (5,16,23). The greedy method runs reasonably fast, but the proposed algorithm further accelerates the optimization by an order of magnitude. Note that we achieved this result while using an even larger set of candidates than the greedy method. For example, the set of candidates for our algorithm had 64^2 elements while the greedy method had 19^2, which is about a factor of 11 times fewer.

Speed versus Accuracy Trade-Off in our Algorithm

The computation time of our algorithm depends on the choice of the parameter, p, the number of the PE location candidates selected by the cumulative correlation test. It determines the trade-off between the computation time and the excitation accuracy. Setting p to its largest value makes our method identical to the modification of the method by (5) and may yield higher excitation accuracy at the expense of computation time. However, we observed from experiments that increasing p above a certain threshold does not generally improve the excitation accuracy significantly. NRMSEs versus p for eight slices are plotted in Fig. 5. A smaller p would reduce computation time, but the curves show some oscillation for $p < 8$. We chose p conservatively ($p = 8$) to avoid exaggerating the computation acceleration of our method.

DISCUSSION

In this article, we presented a fast greedy algorithm for parallel excitation RF pulse design to determine PE locations considering B_0 field inhomogeneity. The original greedy method as implemented (5) and the convex optimization method (4) disregarded off-resonance in the model used for the PE location selection process, which raises two problems. First, it causes model mismatch, potentially selecting ineffective PE locations. In other words, the basis signals associated with the chosen PE locations may be less effective in approximating the desired excitation pattern accurately. Furthermore, it may exaggerate the predicted excitation accuracy estimated in the PE location selection stage, selecting too few PE locations. Second, it requires a heuristic to order the selected PE locations, which may lower excitation accuracy as illustrated in Fig. 3. In contrast, our algorithm jointly determines PE locations and their order by modeling the off-resonance effects during PE location selection and achieved higher excitation accuracy than the conventional methods.

Our algorithm is also very computationally efficient. Both the greedy method (5) and our proposed method ran much faster than the convex method (4), but our method was almost an order of magnitude faster than the greedy method for comparable excitation accuracy. Instead of running orthogonal projections for every candidate PE location as in (5), we culled a few effective candidates with the cumulative correlation test and performed the projection only for these candidates. This approach replaces numerous computationally demanding orthogonal projections with cumulative correlation tests, which are far less demanding because they use efficient operations such as Fast Fourier Transform (FFT) and diagonal matrix multiplications.

Our proposed algorithm is based on an iterative greedy selection procedure that may find a local minimum. The convex method can have an advantage over such greedy approaches from this perspective because it may have a wider search scope for optimal PE location combination. But, the condition for finding the optimal solution is hard to meet and verify as pointed out in (5). Also, in the convex method, one cannot control the computation time with respect to the number of selected PE locations because the termination of the optimization is not directly related to it. On the other hand, in our approach, we can simply terminate the optimization after the required number of PE locations is selected or the

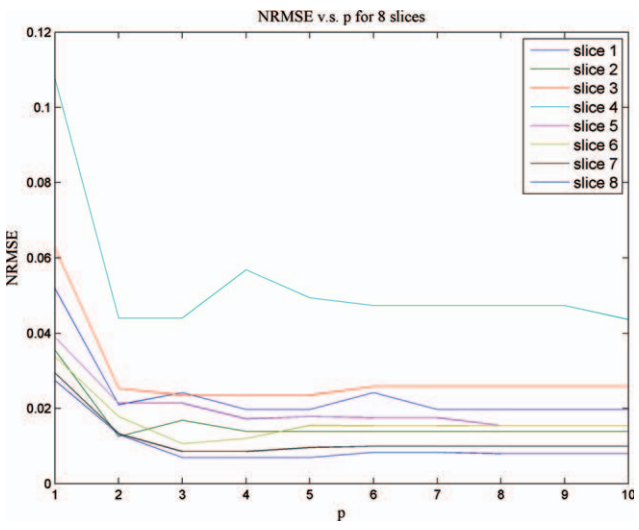

FIG. 5. Normalized excitation errors that our pulse design achieved with different p values for eight slices. As the value of p grows, our method approaches to the greedy method sacrificing the computation time. The plot here shows an approximate L curve shaped form, suggesting that there may be an optimal point for p that has a good balance between computation time and excitation accuracy. [Color figure can be viewed in the online issue, which is available at wileyonlinelibrary.com.]

desired excitation accuracy is achieved. The convex method also requires a pruning technique to cull the specified number of PE locations from the solution. Typically, the locations with largest pulse weights are selected, but in parallel excitation, multiple pulse weights are associated with one PE location, therefore it is not so obvious how to sort them.

In Eq. 1, the basis signal for the mth PE location is modulated by the off-resonance phase, $e^{i2\pi\Delta\omega(x,y)(t_m-T)}$. If the B_0 fieldmap error is denoted as $\varphi(x,y)$, the actual phase modulation becomes $e^{i2\pi(\Delta\omega(x,y)+\varphi(x,y))(t_m-T)}$, whose first-order approximation is $e^{i2\pi\Delta\omega(x,y)(t_m-T)}(1+i2\pi\varphi(x,y)(t_m-T))$. The term $2\pi\varphi(x,y)(t_m-T)$ gives the fractional error. For example, the error for the first PE location in a 5 ms pulse for a 5 Hz error is about 16%. The error is larger for PE locations visited earlier in the k-space. However, our greedy selection approach in a time-reversed order is likely to assign smaller pulse weights for the PE locations selected later (visited earlier in excitation k-space), and this may provide some robustness to B_0 fieldmap errors.

Our cost function for PE location selection did not include a regularizer to control the pulse amplitude, so the pulse weights found during the PE location selection process may violate specific absorption rate (SAR) constraints or the small-tip angle assumption. Our algorithm has not yet been validated with parallel transmit hardware, so it may need to be further limited by coupling between and changes to the B_1 fields as well as restrictions on the peak RF amplitude. A future research topic is to develop methods considering these constraints in the PE location selection process. Also, we expect that greedy algorithms can be further improved by developing methods to refine previously selected PE locations, as suggested in (5) or (24).

CONCLUSION

We have introduced a fast greedy algorithm for determining effective PE locations and their order in the presence of B_0 field inhomogeneity. Our proposed method achieved higher excitation accuracy and faster computation than previous methods. In future work, we plan to extend our method to more complicated applications such as signal recovery for blood oxygenation level dependent functional magnetic resonance imaging (8,19). Also, we will seek an efficient way to incorporate a pulse power regularizer to consider the SAR issue during our optimization.

REFERENCES

1. Saekho S, Yip CY, Noll DC, Boada FE, Stenger VA. Fast-kz three-dimensional tailored radiofrequency pulse for reduced B1 inhomogeneity. Magn Reson Med 2006;55:719–724.
2. Zhang Z, Yip CY, Grissom WA, Noll DC, Boada FE, Stenger VA. Reduction of transmitter B1 inhomogeneity with transmit SENSE slice-select pulses. Magn Reson Med 2007;57:842–847.
3. Zelinski AC, Wald LL, Setsompop K, Alagappan VA, Gagoski BA, Goyal VK, Adalsteinsson E. Fast slice-selective radio-frequency excitation pulses for mitigating $B1^+$ inhomogeneity in the human brain at 7 Tesla. Magn Reson Med 2008;59:1355–1364.
4. Zelinski AC, Wald LL, Setsompop K, Goyal VK, Adalsteinsson E. Sparsity-enforced slice-selective MRI RF excitation pulse design. IEEE Trans Med Imaging 2008;27:1213–1229.
5. Ma C, Xu D, King KF, Liang Z. Joint design of spoke trajectories and RF pulses for parallel excitation. Magn Reson Med 2011;65:973–985.
6. Deng W, Yang C, Alagappan V, Wald LL, Boada FE, Stenger VA. Simultaneous z-shim method for reducing susceptibility artifacts with multiple transmitters. Magn Reson Med 2009;61:255–259.
7. Yang C, Deng W, Stenger VA. Simple analytical dual-band spectral-spatial RF pulses for $B1^+$ and susceptibility artifact reduction in gradient echo MRI. Magn Reson Med 2011;65:370–376.
8. Yoon D, Fessler JA, Gilbert AC, Noll DC. Simultaneous Signal Loss Correction from B1 and B0 Field Inhomogeneity in BOLD fMRI with Parallel Excitation. In: Proc., ISMRM Third International Workshop on Parallel MRI, Santa Cruz, 2009. p 38.
9. Malik S, Larkman DJ, O'Regan DP, Hajnal JV. Subject-specific water-selective imaging using parallel transmission. Magn Reson Med 2010;63:988–997.
10. Setsompop K, Alagappan V, Zelinski AC, Potthast A, Fontius U, Hebrank F, Schmitt F, Wald LL, Adalsteinsson E. High-flip-angle slice-selective parallel RF transmission with 8 channels at 7 T. J Magn Reson 2008;195:76–84.
11. Grissom WA, Kerr AB, Stang P, Scott GC, Pauly JM. Joint Design of Large-Tip-Angle RF and Gradient Waveforms in Parallel Excitation. In: Proc., ISMRM Third International Workshop on Parallel MRI, Santa Cruz, 2009; p 12.
12. Yip CY, Fessler JA, Noll DC. Iterative RF pulse design for multidimensional, small-tip-angle selective excitation. Magn Reson Med 2005;54:908–917.
13. Grissom WA, Yip CY, Zhang Z, Stenger VA, Fessler JA, Noll DC. Spatial domain method for the design of RF pulses in multicoil parallel excitation. Magn Reson Med 2006;56:620–629.
14. Pauly JM, Nishimura DG, Macovski A. A k-space analysis of small-tip-angle excitation. Magn Reson Med 1989;81:43–56.
15. Chen D, Bornemann F, Vogel MW, Sacolick LI, Kudielka G, Zhu Y. Sparse Parallel Transmit Pulse Design using Orthogonal Matching Pursuit Method. In: Proc., ISMRM, 17th Annual Meeting, Honolulu, 2009. p 171.
16. Yoon D, Gilbert AC, Fessler JA, Noll DC. Fast Selection of Phase Encoding Locations in Parallel Excitation. In: Proc., ISMRM, 17th Annual Meeting, Honolulu, 2009. p 2595.
17. Pati YC, Rezaiifar R, Krishnaprasad PS. Orthogonal Matching Pursuit: Recursive Function Approximation with Applications to Wavelet Decomposition. Proceedings of 27th Asilomar Conference on Signals, Systems and Computers, Vol. 1, Pacific Grove, CA, 1993. pp 40–44.
18. Reeves SJ, Zhao Z. Sequential algorithms for observation selection. IEEE Trans Signal Process 1999;47:123–132.
19. Yip CY, Fessler JA, Noll DC. Advanced three-dimensional tailored RF pulse for signal recovery in T2*-weighted functional magnetic resonance imaging. Magn Reson Med 2006;56:1050–1059.
20. Tropp JA, Gilbert AC, Strauss MJ. Algorithms for simultaneous sparse approximation. Part I: greedy pursuit. Signal Processing 2006; 86:572–588.
21. Kurpad KN, Boskamp EB, Wright SM. A Parallel Transmit Volume Coil with Independent Control of Currents on the Array Elements. In: Proc., ISMRM 13th Scientific Meeting, Miami Beach, 2005. p 16.
22. Wright SM. 2D full-wave modeling of SENSE coil geometry factors at high fields. In: Proc., ISMRM 10th Scientific Meeting, Honolulu, 2002. p 854.
23. Chen SS, Donoho DL, Saunders MA. Atomic decomposition by basis pursuit. SIAM J Sci Comput 1998;20:33–61.
24. Needell D, Tropp JA. CoSaMP: iterative signal recovery from incomplete and inaccurate samples. Appl Comput Harmon Anal 2008;26: 301–321.